

Absolute H density in an RF driven Ar + H₂O atmospheric pressure plasma jet by two photon absorption laser induced fluorescence

V. S. S. K. Kondeti and P. J. Bruggeman

Department of Mechanical Engineering, University of Minnesota, Minneapolis, USA

Abstract: The absolute H density generated by an Ar + 0.27% H₂O radio frequency driven time-modulated atmospheric pressure plasma jet was measured using two photon absorption laser induced fluorescence. The highest H density measured in the plasma effluent was $9 \times 10^{15} \text{ cm}^{-3}$ and is an order of magnitude higher than the maximum OH density. The corresponding dissociation degree of water is $\sim 21\%$. The high radical density leads to a fast reduction in the H density in the jet effluent with increasing distance from the APPJ nozzle. While the plasma jet is modulated at 20 kHz, the H density generated by the modulated RF plasma jet is independent of time for practical relevant treatment distances in excess of 6 mm from the plasma jet nozzle.

Keywords: Atomic H density, TaLIF, atmospheric pressure plasma jet.

1. Introduction

Atmospheric pressure plasma jets (APPJs) have a wide range of applications such as nanoparticle synthesis, processing of materials and disinfection [1]. These applications are made possible by the generation of a wide variety of highly reactive species at close-to-room temperature. APPJs are typically operated with argon or helium as feed gas often enriched with a small admixture of a molecular gas such as oxygen, air and water vapor to enhance the production of highly reactive H, O and OH radicals. Recent experiments and models showed that the density of H generated in a high electron density plasma filament ($> 10^{16} \text{ cm}^{-3}$) can be two orders of magnitude higher than the OH density [2]. However, in diffuse, low electron density plasmas ($\sim 10^{12} \text{ cm}^{-3}$), the H and OH density is similar [3]. In this work, we investigate the H density in a high-power density radio frequency (RF) jet that has an intermediate electron density ($\sim 10^{14} \text{ cm}^{-3}$). The absolute H density is measured by two photon absorption laser induced fluorescence (TaLIF).

2. Experiment

A well characterized RF driven APPJ was used in this work [4]. A 1 mm diameter tungsten needle electrode was powered by a RF power source (13.6 MHz) that was operated at 20 kHz modulation with a duty cycle of 20%. Argon with 0.27 % of H₂O (1.5 slm) flowed through a 2 mm ID \times 3 mm OD quartz tube that surrounds the needle electrode. The plasma jet was operated at atmospheric pressure in open air and the average plasma dissipated power was maintained at 2.5 W.

The H density in the plasma was measured by TaLIF. A pump-dye laser system generates photons at 205.08 nm as described in detail in Ref. [4]. A combination of two such photons excite the ground state H atoms from $1s \ ^2S_{1/2}$ state to $3d \ ^2D_{3/2, 5/2}$ states. The de-excitation from this excited state to $2p \ ^2P_{1/2, 3/2}$ state results in fluorescence at 656.28 nm. This fluorescence was captured by an

intensified charge coupled camera (ICCD). A bandpass filter centred at 656 nm was used to detect the fluorescing photons. The absolute H density was calibrated using a known concentration of krypton gas. The ground state Kr atoms are excited from $4p^6 \ ^1S_0$ to $5p' \ [3/2]_2$ state. The de-excitation to $5s \ [3/2]_1$ state emits fluorescence at 587.1 nm. The fluorescence was captured with the combination of a spectrometer and an ICCD camera. The absolute H density is calculated using the following equation.

$$n_H = n_{Kr} \frac{\sigma_{Kr}^{(2)} a_{Kr}}{\sigma_H^{(2)} a_H} \left(\frac{h\nu_H}{h\nu_{Kr}} \right)^2 \frac{g_{Kr} S_H}{g_H S_{Kr}} \Upsilon \quad (1)$$

Where 'n' is the density, 'σ' the two photon absorption cross section, 'a' the branching ratio, 'hν' the photon energy, 'g' the branching ratio, 'S' the fluorescence intensity and 'Υ' the detection efficiency of the system at the observed wavelengths. It is assumed that the main quencher of the excited H-state is Ar. The subscripts H and Kr refer to atomic hydrogen and krypton, respectively. The calculation of the variables used in the calibration can be found in Ref. [5]. The gas temperature was measured by Rayleigh scattering.

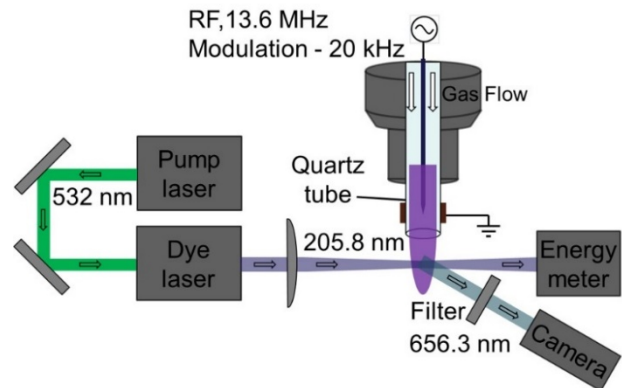


Figure 1. Schematic of the two photon absorption laser induced fluorescence measurements.

3. Results

The plasma jet is operated at 20 kHz modulation with a duty cycle of 20%. Hence, the discharge is on for 10 μs and off for 40 μs . The fluorescence intensity increases with the start of the RF pulse close to the plasma jet nozzle at 1 mm distance from the nozzle while it decays after the end of the 10 μs RF pulse (Figure 2). However, at a distance of 6 mm from the APPJ nozzle, the fluorescence intensity does not vary with respect to the RF pulse. For several applications such as surface processing which are typically performed at larger distances from the plasma jet nozzle, the H density in this APPJ does not vary with time.

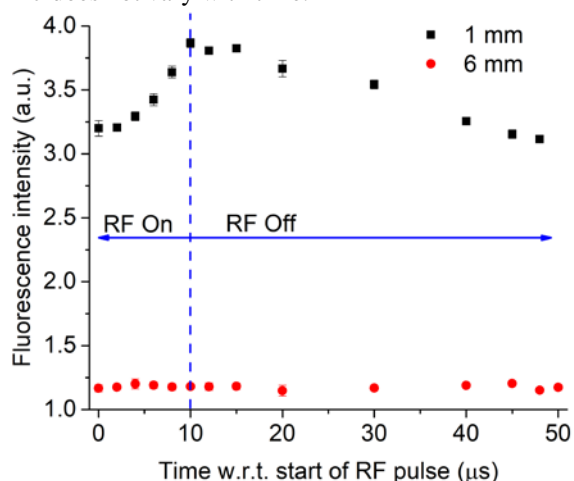


Figure 2. Variation of H density as a function of time for one RF modulation duty cycle.

The variation in the gas temperature of the APPJ with the increase in the distance from the APPJ nozzle is shown in Figure 3. The gas temperature close to the APPJ nozzle is 480 K while it reduces to 350 K at 15 mm from the APPJ nozzle. Figure 3 also shows the variation of absolute H density with the increase in distance from the RF jet nozzle. The maximum H density measured was about $9 \times 10^{15} \text{ cm}^{-3}$ at 0.5 mm from the plasma jet nozzle. This corresponds to a dissociation degree of $\sim 21\%$ of the feed gas H_2O_2 which is anticipated to be even higher in the core of the discharge. This suggests that a very high-power density inside the jet that leads to a larger dissociation of the H_2O inside the jet. The production of H is expected to be mainly in the active discharge while it is transported downstream by the gas flow. Measured OH densities in the same jet (although with shielding co-flow) did not exceed 10^{15} cm^{-3} [6]. This is consistent with the plug flow model of the jet which showed that the OH density generated by this APPJ is one order of magnitude lower than the H density measured in this work [7]. The model also shows that the O density is of the order of 10^{14} cm^{-3} . The gas phase H_2O_2 concentration in the far effluent estimated from the jet by a volumetric increase in the liquid phase H_2O_2 concentration treated by the APPJ is approximately $3 \times 10^{14} \text{ cm}^{-3}$ [8]. The decay constant of the decrease in H density with the distance from the APPJ nozzle is approximately 4 mm and the density of H

reduces by an order of magnitude at 8 mm. The unexpected fast reduction in the density of H with the increasing distance from the APPJ nozzle is due to the reactions of H with H and OH radicals.

4. Conclusion

The absolute H density generated by an RF driven APPJ was measured by two photon absorption laser induced fluorescence. The H density varies with time during one RF modulation cycle close to the APPJ nozzle while it is nearly constant further away from the APPJ nozzle. The highest H density measured in the APPJ was $9 \times 10^{15} \text{ cm}^{-3}$. The measured H density was found to be an order of magnitude higher than the OH density for the plasma source. A large reduction in the H density with the increase in distance from the APPJ nozzle is due to the recombination of H with H and OH radicals.

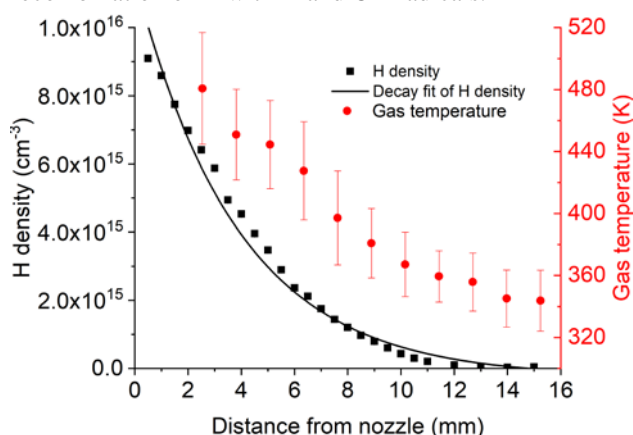


Figure 3. H density and gas temperature as a function of the distance from the APPJ nozzle, 2 μs after the end of the plasma on phase in the modulation cycle.

5. Acknowledgement

This work is supported by the US Department of Energy through the Plasma Science Centre (DE-SC0001939) and the Office of Fusion Energy Sciences (DE-SC0016053).

6. References

- [1] I. Adamovich *et al.*, J. Phys. D. Appl. Phys., **50**, 323001 (2017).
- [2] Y. Luo, A. M. Lietz, S. Yatom, M. J. Kushner & P. J. Bruggeman, J. Phys. D. Appl. Phys., **52**, 044003 (2019).
- [3] D. X. Liu *et al.*, Plasma Sources Sci. Technol., **19**, 2 (2010).
- [4] V. S. S. K. Kondeti, U. Gangal, S. Yatom & P. J. Bruggeman, J. Vac. Sci. & Tech. A, **6**, 35 (2017).
- [5] S. Yatom, Y. Luo, Q. Xiong and P. J. Bruggeman, J. Phys. D. Appl. Phys., **50**, 41 (2017).
- [6] P. Luan, V. S. S. K. Kondeti, A. Knoll, P. J. Bruggeman & G. S. Oehrlein, Submitted (2019).
- [7] K. Wende, *et al.*, Biointerphases, **10**, 2 (2015).
- [8] H. Taghevai, V. S. S. K. Kondeti & P. J. Bruggeman, submitted (2018).